Correspondence

Initial Phantom Validation of Minute Roughness Measurement Using Phase Tracking for Arterial Wall Diagnosis Non-Invasively *In Vivo*

Magnus Cinthio, Hideyuki Hasegawa, and Hiroshi Kanai

***Abstract*—To detect minute roughness, we utilized the phase change that occurs in a radio frequency echo from the rough surface of an object during its lateral motion. The new method was optimized and validated using saw-tooth-shaped silicone phantoms sized from 13 to 33 μm; results were compared to those obtained using a confocal laser scanning microscope.**

I. Introduction

Atherosclerosis is an inflammatory disease affecting the arteries, which accumulate sub-endothelial lipid-laden foam cells and associated T lymphocytes and form non-stenotic fatty streaks [1]. When the fatty streaks progress, it is highly likely that the inner surface of arterial wall becomes uneven before it becomes thick. However, as far as we know, this has never been investigated. We believe that by measuring the unevenness of the inner structures of the arterial wall, i.e., the defect of the endothelium, it may be possible to detect signs of atherosclerosis earlier than using current methods.

To obtain an indirect measure of the unevenness, Pedersen *et al.* have developed an angular spectrum-based formulation method [2]–[4]. Zhang *et al.* have developed a 3-D ultrasound system with the ability to extract surfaces using radial basis functions. This method produces realistic surfaces with a high level of detail [5], however, the measurement error was in the millimeter range. Gunarathne *et al.* have developed an ultrasonic spectroscopic technique to measure the gross surface texture of non-medical materials. They introduced a roughness coefficient that specified the texture on a quantitative basis [6].

Non-invasive *in vivo* examination of the common carotid artery and other superficial arteries requires ultrasound frequencies of 5 to 15 MHz. At these frequencies, the magnitude of early roughness is smaller than the wavelength of the RF signal. To further complicate the measurement, the arterial wall moves both radially and longitudinally during the cardiac cycle [7]–[10]. One way to obtain information regarding roughness which is less than the wavelength is to utilize the phase of the RF echo. The most obvious way is to compare the phase information between several beams along the surface in one frame. This approach would probably work well in a water tank where there are no differences in attenuation or in sound velocity between the ultrasonic beams. However, when using this approach in arterial characterization, a major problem arises; the small variation in the speed of sound between different beams, which is highly likely, introduces aberration error. For example, if the object of interest is 30 mm below the transducer and the speed of sound varies only 0.1% between two beams, this causes a difference of 0.1% between the distances to the surface. However, this difference corresponds to 30 μm, and in this context 30 μm is much greater than the micro-scale roughness we are interested in determining. Fig. 1 shows the setup and the resulting ultrasonic B-mode images of a flat glass surface (usually used for optical microscopes) with and without porcine cutlet placed between the transducer and the glass surface. As can be seen in the figure, the aberration errors make it impossible to estimate the surface profile (highly flat in this case) by comparing the depth positions of the surface using adjacent ultrasonic beams.

Therefore, Arihara *et al.* suggested a one-beam approach, which utilizes the fact that the phase of an RF echo changes because of the change in distance (Fig. 2) when a rough object is moved laterally. They validated the approach using a silicone phantom moving laterally in a water tank [11]. The measurement error was in the micrometer range.

To further extend this approach for arterial characterization, we recently proposed a method [12] by which the roughness of the inner layer of the arterial wall can be measured by combining precise measurement of the axial motion using phase tracking [11], [13] with measurement of the natural longitudinal movement [9] of the arterial wall. The aim of the present study was to further examine this new method's ability and to validate it using silicone phantoms, comparing our results with those obtained with a confocal laser scanning microscope.

II. Material and Methods

A. The Algorithm

Let $f(m\Delta x, k\Delta y, n)$ $(n = 1, 2, \ldots, N)$ denote a cineloop consisting of N image frames, where Δx and Δy are the lateral and axial spacing of sampled points, respectively, and m and k are ultrasonic beam number and sampled point number, respectively, corresponding to a position

Manuscript received November 22, 2010; accepted January 24, 2011. This study was supported by the Japanese Society for the Promotion of Science and the Swedish Research Council.

M. Cinthio is with Electrical Measurements, Faculty of Engineering, LTH, Lund University, Lund, Sweden (e-mail: magnus.cinthio@elmat.lth.se).

H. Hasegawa and H. Kanai are with the Department of Biomedical Engineering, Graduate School of Biomedical Engineering, Tohoku University, Sendai, Japan.

H. Hasegawa and H. Kanai are also with the Department of Electronic Engineering, Graduate School of Engineering, Tohoku University, Sendai, Japan.

Digital Object Identifier 10.1109/TUFFC.2011.1879

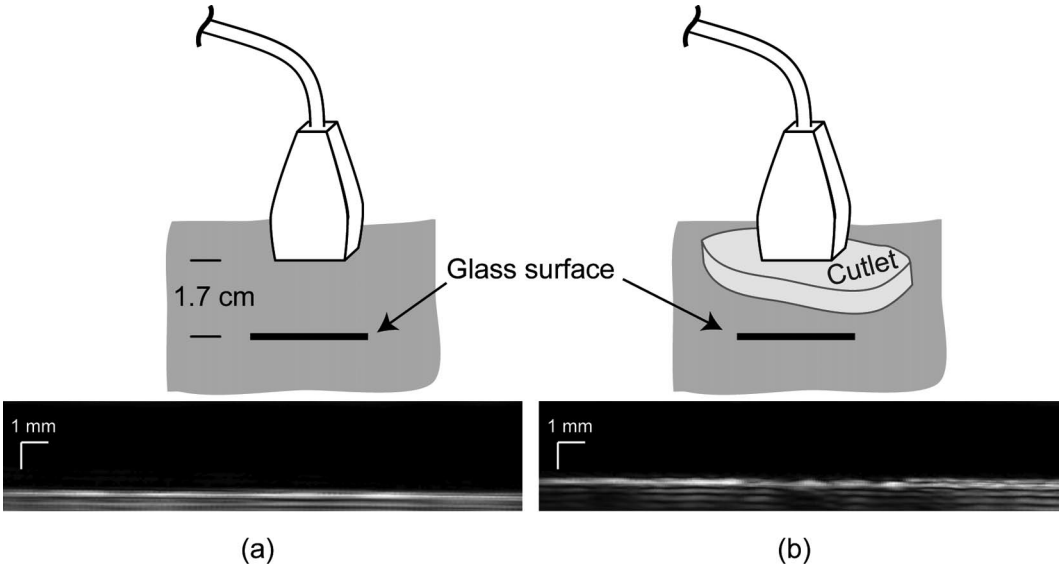

Fig. 1. The setup and the resulting ultrasonic B-mode image of a flat glass surface (a) without and (b) with a 1-cm-thick porcine cutlet placed between the transducer and the glass surface. Note the severe aberration errors in (b) that make it impossible to compare adjacent ultrasonic beams to estimate the roughness of the surface.

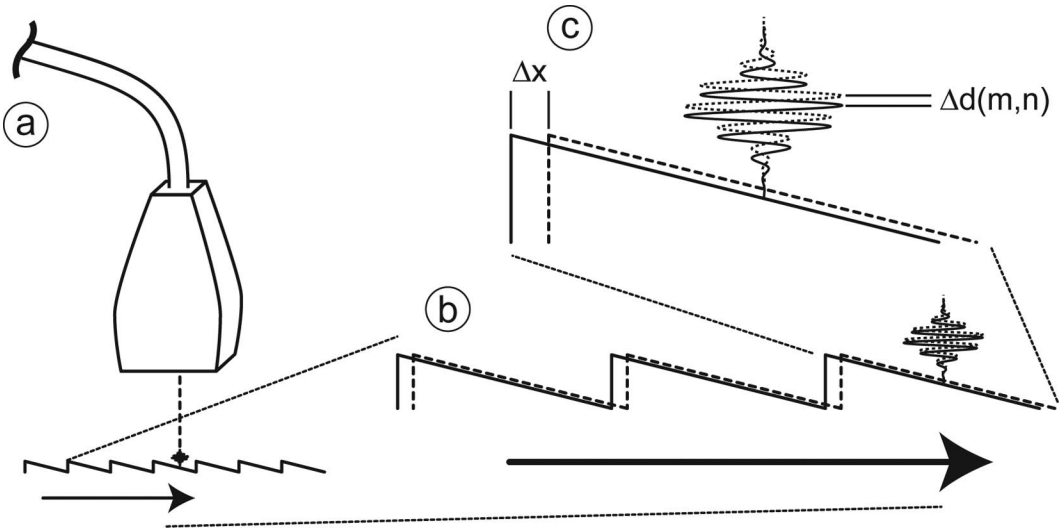

Fig. 2. Schematic of roughness measurement utilizing the phase of an ultrasonic beam. (a) The phase is measured at one position during lateral movement of the object. The lateral movement is measured using 2-D high-resolution echo-tracking. (b) The object and the resulting echoes at two successive frames are shown enlarged. (c) One enlarged saw tooth at two successive frames and the resulting echoes are shown. Δx = the lateral displacement between two frames. $\Delta d(m,n)$ = the resulting phase change between two frames.

in the lateral x and axial y directions in the image plane. When a rough surface is moved laterally, as in the case of an arterial wall [10], the corresponding time delay of an echo becomes different (Fig. 2). This change in time delay can be detected as an axial displacement $d(m\Delta x, n)$ at beam position $m\Delta x$ in frame n using a phase-sensitive axial displacement estimator [13]. When the artery is scanned in the longitudinal direction, the axial and lateral movements correspond to the arterial radial and longitudinal directions, respectively.

By defining the axial displacements induced by surface roughness as $d_s(m\Delta x, n)$ and the global motion that arises from transducer motion, leaning surfaces, and the change in lumen diameter as $d_g(m\Delta x, n)$, the axial displacement $d(m\Delta x, n)$ estimated by the phase-sensitive axial displacement estimator is expressed as follows:

$$d(m\Delta x, n) = d_s(m\Delta x, n) + d_g(m\Delta x, n). \tag{1}$$

The axial displacements induced by surface roughness have a high spatial frequency, whereas axial transducer motion, as well as a leaning surface moving longitudinally, introduces axial motion that is equal at different positions laterally, i.e., a spatial frequency close to zero. Regarding the lumen diameter change, the pulse-wave velocity in the artery is typically 5 m/s and the main frequency components of the pulsation of the artery are less than 10 Hz. This corresponds to a wavelength of the pulse-wave that is

longer than 50 cm. Because the longitudinal movement of the arterial wall is less than 2 mm and the maximum scanning area is 20 mm, the region of interest can be considered short. Furthermore, the viscoelastic properties of the arteries in very early-stage atherosclerosis are considered to be homogeneous. Thus, we can assume that the axial movement induced by pulsation of the heart does not depend on the lateral position, i.e., spatial frequency is also close to zero in the case of the change in diameter.

Measured displacement $d(m\Delta x, n)$ can be differentiated with respect to lateral position x as follows:

$$\frac{\partial d(m\Delta x,n)}{\partial x} \approx \frac{d((m+1)\Delta x,n) - d(m\Delta x,n)}{\Delta x} = \Delta d(m\Delta x,n). \tag{2}$$

By applying the Fourier transform to (2), the following relationship is obtained:

$$\begin{aligned} &\frac{1}{\Delta x}\mathrm{FT}_x[d((m+1)\Delta x,n) - d(m\Delta x,n)] \\ &\quad = \frac{1}{\Delta x}\{\exp(j2\pi f_x \Delta x) - 1\} \cdot \mathrm{FT}_x[d(m\Delta x,n)] \\ &\quad = H(f_x) \cdot \mathrm{FT}_x[d(m\Delta x,n)], \end{aligned} \tag{3}$$

where $\mathrm{FT}_x[\cdot]$ is the Fourier transform with respect to x and $H(f_x) = \{\exp(j\,2\pi\,f_x\,\Delta x - 1) - 1\}/\Delta x$ is the transfer function of the differential operation. Obviously, $|H(f_x)|$ is zero at $f_x = 0$, i.e., spatial high-pass filtering. Therefore, after the differentiation of $d(m\Delta x, n)$ with respect x, global motion $d_g(m\Delta x, n)$ in (1) can be removed, and only the displacement $d_s(m\Delta x, n)$ induced by surface roughness remains. However, the differentiated displacement $\Delta d(m\Delta x, n)$ is dimensionless. To obtain the surface profile (roughness) in meters, differentiated displacement $\Delta d(m\Delta x, n)$ is integrated with respect to lateral position x as follows:

$$\begin{aligned} d_{\Delta m}(m\Delta x,n) &= \sum_{i=m-\Delta m}^{m+\Delta m} \Delta x \cdot \Delta d(i\Delta x,n) \\ &= d_{s,\Delta m}(m\Delta x,n) \equiv d_{s,\Delta m}(m,n). \end{aligned} \tag{4}$$

From (4), it can be seen that the axial displacement $d_{s,\Delta m}(m, n)$ induced by the surface roughness can be obtained from $d(m\Delta x, n) \equiv d(m, n)$ measured by ultrasound after spatial differentiation and integration. In the spatial high-pass filtering procedure, $\Delta m = 1$ was used, i.e., to obtain axial displacement induced by the roughness in one position, three ($2\Delta m$+1) adjacent scan lines were differentiated and integrated.

The $d_{s,\Delta m}(m, n)$ corresponds to the change in height of a surface at beam m from the height at frame 0, induced by the lateral displacement $l(m, n)$. The lateral position x_n on the surface measured by beam m in frame n can be obtained by the lateral displacement $l(m, n)$. Therefore, by estimating the lateral displacement $l(m, n)$ using a high-resolution echo-tracking method based on cross-correlation [10], the roughness profile $r(x_n)$ of the surface is obtained as follows:

$$r(x_n) = r(l(m,n)) = d_{s,\Delta m}(m,n). \tag{5}$$

B. Measurement System

All of the measurements were performed using a modified commercial ultrasound system (Prosound II, Aloka, Tokyo, Japan). The system was equipped with a 10-MHz linear array transducer 40 mm in width. It was desirable to achieve the best possible spatial and temporal quantification and, thus, the number and interval of scan lines were set as small as possible, resulting in a frame rate of 70 Hz and scan line intervals of 100 μm. These settings allowed a lateral image width of 20 mm. The sampling frequency of RF echoes was 40 MHz.

C. Algorithm Evaluation

To confirm the need for the spatial filtering, we conducted an experiment on a flat surface with 1-cm-thick porcine cutlet between the transducer and the surface-of-interest, which introduced distinct aberration error. Six replicates were conducted on a flat glass surface with porcine cutlet between the transducer and the glass surface.

The method was evaluated using three silicone phantoms. The silicone phantoms were produced using metallic molds which were manufactured using a milling machine. To investigate the ability of the method on both steps and slopes, the molds were saw-tooth-shaped. Ten saw teeth, whose heights were designed to be 13, 23, and 33 μm, were milled on the top of the molds, with the width of one tooth being 0.5 mm.

Reference measurement of the phantoms was made by a confocal laser scanning microscope (VK-9700, Keyence, Tokyo, Japan). The resolution of the measurement using the laser system was 14 nm.

The repeatability between measurements and the accuracy of the proposed method was analyzed using the method of Bland and Altman [14].

III. Results

Fig. 1(b) shows an ultrasonic B-mode image of a flat glass surface when a porcine cutlet was placed between the transducer and the glass surface. The aberration errors make it impossible to compare ultrasonic beams beside each other to estimate the roughness of the surface. The roughness of the glass surface estimated during its lateral movement using our novel approach was 0.43 μm [standard deviation (SD) 0.28 μm].

Fig. 3(a) shows a B-mode image of the phantom with 33-μm saw teeth. As can be seen in Fig. 3(a), it is difficult to measure surface roughness quantitatively using conventional B-mode images. By using the phase-sensitive

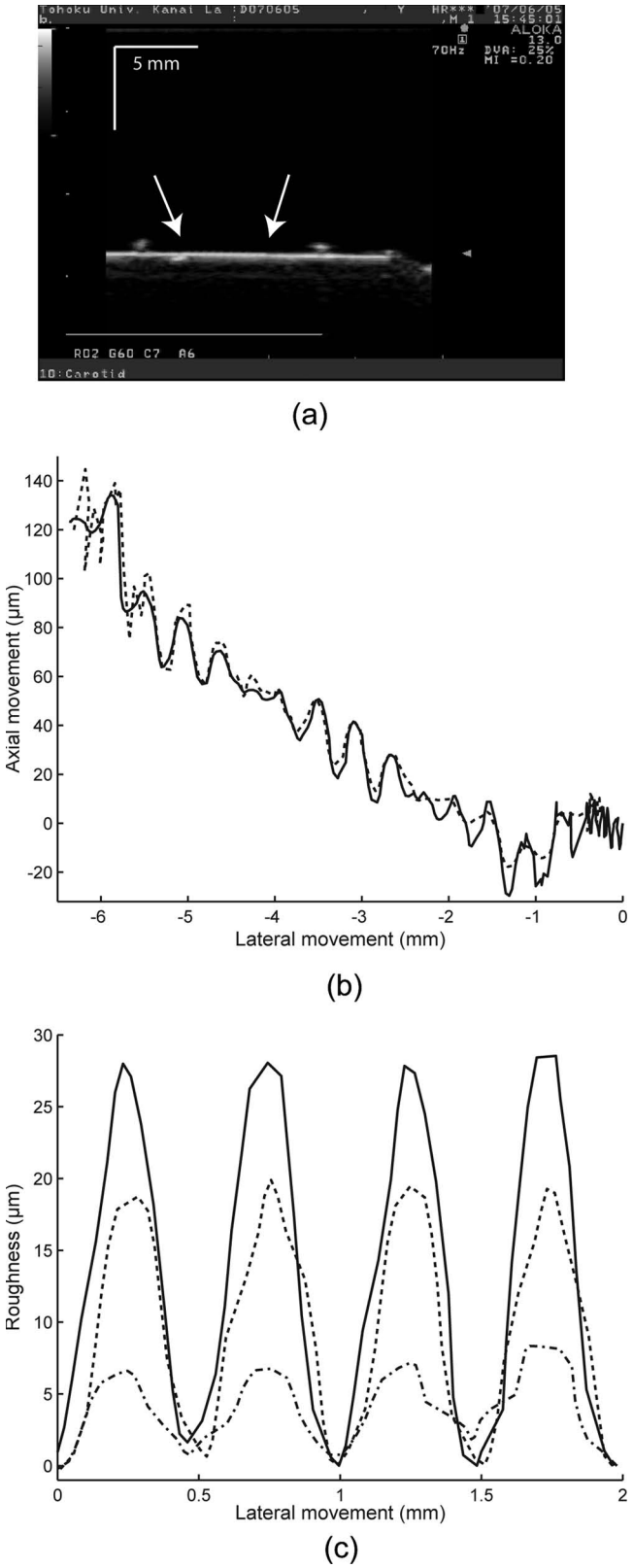

Fig. 3. (a) Ultrasonic image of the 33-μm phantom with no aberrating layer between the transducer and the phantom. The phantom is shown between the arrows. (b) The measured axial displacement of the phantom surface against the measured lateral movement of the phantom at one beam in the forward and backward (dashed) direction, respectively, during one measurement on the 33-μm-phantom. Note the different scales on the axes. (c) Resulting roughness curves of four saw teeth after spatial filtering for the 33-μm phantom, the 23-μm phantom (dashed), and the 13-μm phantom (dashed-dotted), respectively.

displacement estimator [13], the axial displacements of the surfaces of the 13-, 23-, and 33-μm phantoms during their lateral motion were measured as shown in Fig. 3(b). Because of difficulty in obtaining exact 90° alignment between transducer and phantom, a global displacement up to hundreds of micrometers occurred axially. By applying spatial filtering, the roughness curves of four saw teeth at one beam during the lateral motion were obtained for all three phantoms, as shown in Fig. 3(c).

The optimal size and position of the correlation kernel used for estimation of the axial displacement was determined by repetitive measurements of the phantom so that the difference between the surface profile measured by ultrasound and that measured by the confocal laser microscope was minimized. The size and position of the kernel was optimized to be seven samples (0.13 mm) and nine samples (0.17 mm) closer to the ultrasonic probe than the peak position of the envelope of an echo from the surface. The results of the roughness estimations obtained using the optimized kernel size and position are summarized in Table I. For the repetitive measurements, the systematic and random differences from the results obtained by the confocal laser microscope were −0.39 μm and 0.86 μm, respectively. The mean difference between the results obtained by ultrasound and laser was −7.6 μm (SD 2.8) for the 13-μm phantom; −6.8 μm (SD 2.3) for the 23-μm phantom and −6.1 μm (SD 3.4) for the 33-μm phantom.

IV. Discussion

We have recently shown the possibility of measuring a 12-μm-step surface profile with a measurement error in the micrometer range using the relative phase change of one ultrasonic beam using a phase-tracking algorithm when the object is moved laterally. In the present study, this concept was extended by a simultaneous measurement of lateral movement of the object using an echo-tracking algorithm on the same cineloop to make it possible to measure the roughness of the arterial wall. As a result, detection of a small change in height, [Fig. 3(b)] not noticeable in a conventional B-mode image by the naked eye, was shown to be possible. Furthermore, accurate and repeatable measurement of the height and width of saw tooth profiles was achieved, which shows promise for both medical and non-medical applications.

As described previously, there was a systematic error of 7 μm (smaller than the true value). One of the reasons for this may have been the width of the ultrasonic beam. The lateral width at half-maximum of the ultrasonic beam used was about 0.8 mm, slightly larger than the pitch of the saw teeth. Therefore, an echo signal obtained at a beam position coinciding with the peak of a saw tooth contains a weak echo from a dip in addition to the echo from the peak. In this case, the difference in phases of echo signals obtained at beam positions coinciding with a peak and a dip decreases, resulting in the underestimation

TABLE I. SUMMARY OF ULTRASONIC AND LASER MEASUREMENTS OF 13-, 23-, AND 33-μM PHANTOMS.

	Ultrasound				Laser
	Roughness (μm)		Width (μm)		Roughness (μm)
Phantom	Mean	SD_{teeth}	Mean	SD_{teeth}	Mean
13 μm	6.3 (SD 0.1)	2.7 (SD 0.0)	507 (SD 9)	62 (SD 6)	13.9 (SD 1.5)
23 μm	16.7 (SD 1.2)	3.3 (SD 0.1)	493 (SD 3)	33 (SD 4)	23.5 (SD 2.1)
33 μm	24.5 (SD 1.1)	3.8 (SD 0.1)	494 (SD 3)	26 (SD 5)	30.6 (SD 1.8)

Mean: the mean and the standard deviation of six measurements. SD_{teeth}: the mean and the standard deviation of the standard deviation within one measurement.

of the roughness. This effect would limit the measurable lateral pitch of the roughness. Further experiments on different phantom widths and lateral velocities, non-periodic roughness shapes, more realistic phantoms with 2-D patterns and scatterers should be conducted; thereafter the proposed method should be tested *in vivo*.

The spatial differentiation and integration operations remove the global motion of the arterial wall during the cardiac cycle by assuming that the global motion is constant among the scan lines used for differentiation and integration. It is advisable to set the length (the number of scan lines) for spatial filtering to be as narrow as possible to meet this assumption. Therefore, three scan lines were used in the spatial high-pass filtering procedure. In this study, we did not correct for the scan velocity, i.e., the three beams were not scanned simultaneously. This small time delay when the different beams are scanned may have introduced the small measurement error shown in the experiment on the flat glass surface. Further investigation needs to clarify this and its possible importance in roughness measurements.

In our experiments, we have shown that the spatial high-pass filter can handle leaning surfaces and global movement of tens of micrometers (which especially occurred when the direction of motion of the phantom does not perfectly coincide with the lateral direction). However, for the *in vivo* investigation, we also need to handle global movement which has a limited pulse-wave velocity. This makes the diameter change, i.e., the global movement starts at different times at different ultrasonic beams. To overcome this potential problem, it might be necessary to avoid measurement of the roughness at early systole.

V. CONCLUSION

This study showed that by combining measurement of the axial motion using phase tracking and lateral motion using high-resolution 2-D cross-correlation, a small change of 100 μm in height, not noticeable to the naked eye, can be detected. It was also shown that by applying spatial high-pass filtering to remove the global motion, the height and width of saw-tooth profiles on silicone phantoms can be accurately and repeatedly measured.

REFERENCES

[1] R. Ross, "Mechanisms of disease: Atherosclerosis—An inflammatory disease," *N. Engl. J. Med.*, vol. 340, no. 2, pp. 115–126, 1999.

[2] B. J. Dean and P. C. Pedersen, "Angular spectrum based formulation of rough surface with applications to surface characterization," in *Proc. IEEE Ultrasonics Symp.*, 1996, pp. 693–696.

[3] J. E. Wilhjelm, P. C. Pedersen, S. M. Jacobsen, and K. Martinsen, "Echo signal from rough planar interfaces influence of roughness, angle, range and transducer type," in *Proc. IEEE Ultrasonics Symp.*, 1998, pp. 1839–1842.

[4] J. E. Wilhjelm, P. C. Pedersen, and S. M. Jacobsen, "The influence of roughness, angle, range, and transducer type on the echo signal from planar interfaces," *IEEE Trans. Ultrason. Ferroelectr. Freq. Control*, vol. 48, no. 2, pp. 511–521, 2001.

[5] W. Y. Zhang, R. N. Rohling, and D. K. Pai, "Surface extraction with a three-dimensional freehand ultrasound system," *Ultrasound Med. Biol.*, vol. 30, no. 11, pp. 1461–1473, 2004.

[6] G. P. P. Gunarathne and K. Christidis, "Measurements of surface texture using ultrasound," *IEEE Trans. Instrum. Meas.*, vol. 50, no. 5, pp. 1144–1148, 2001.

[7] M. Persson, Å. R. Ahlgren, A. Eriksson, T. Jansson, H. W. Persson, and K. Lindström, "Non-invasive measurement of arterial longitudinal movement," in *Proc. IEEE Ultrasonics Symp.*, 2002, vol. 2, pp. 1783–1786.

[8] M. Persson, Å. Rydén Ahlgren, T. Jansson, A. Eriksson, H. W. Persson, and K. Lindström, "A new non-invasive ultrasonic method for simultaneous measurements of longitudinal and radial arterial wall movements: First *in vivo* trial," *Clin. Physiol. Funct. Imaging*, vol. 23, no. 5, pp. 247–251, 2003.

[9] M. Cinthio, Å. R. Ahlgren, T. Jansson, A. Eriksson, H. W. Persson, and K. Lindström, "Evaluation of an ultrasonic echo-tracking method for measurements of arterial wall movements in two dimensions," *IEEE Trans. Ultrason. Ferroelectr. Freq. Control*, vol. 52, no. 8, pp. 1300–1311, 2005.

[10] M. Cinthio, Å. R. Ahlgren, J. Bergkvist, T. Jansson, H. W. Persson, and K. Lindström, "Longitudinal movements and resulting shear strain of the arterial wall," *Am. J. Physiol. Heart Circ. Physiol.*, vol. 291, no. 1, pp. H394–H402, 2006.

[11] C. Arihara, H. Hasegawa, and H. Kanai, "Accurate ultrasonic measurement of surface profile using phase shift of echo and inverse filtering," *Jpn. J. Appl. Phys.*, vol. 45, no. 5B, pp. 4727–4731, 2006.

[12] M. Cinthio, H. Hasegawa, and H. Kanai, "Minute roughness measurement using phase tracking for arterial wall diagnosis non-invasively *in vivo*," in *Proc. IEEE Ultrasonics Symp.*, 2007, pp. 997–1000.

[13] H. Kanai, Y. Koiwa, and J. Zhang, "Real-time measurements of local myocardium motion and arterial wall thickening," *IEEE Trans. Ultrason. Ferroelectr. Freq. Control*, vol. 46, no. 5, pp. 1229–1241, 1999.

[14] J. M. Bland and D. G. Altman, "Statistical methods for assessing agreement between two methods of clinical measurement," *Lancet*, vol. 327, no. 8476, pp. 307–310, 1986.